Hindawi Publishing Corporation
International Journal of Rheumatology
Volume 2012, Article ID 609795, 9 pages
doi:10.1155/2012/609795

Clinical Study

Immunohistochemical Characteristics of IgG4-Related Tubulointerstitial Nephritis: Detailed Analysis of 20 Japanese Cases

Mitsuhiro Kawano,[1] Ichiro Mizushima,[1] Yutaka Yamaguchi,[2] Naofumi Imai,[3] Hitoshi Nakashima,[4] Shinichi Nishi,[5] Satoshi Hisano,[6] Nobuaki Yamanaka,[7] Motohisa Yamamoto,[8] Hiroki Takahashi,[8] Hisanori Umehara,[9] Takao Saito,[4] and Takako Saeki[10]

[1]*Division of Rheumatology, Department of Internal Medicine, Kanazawa University Hospital, Kanazawa, Ishikawa 920-8641, Japan*
[2]*Yamaguchi's Pathology Laboratory, Matsudo, Chiba 270-2231, Japan*
[3]*Division of Clinical Nephrology and Rheumatology, Niigata University Graduate School of Medical and Dental Sciences, Niigata 951-8510, Japan*
[4]*Division of Nephrology and Rheumatology, Department of Internal Medicine, Faculty of Medicine, Fukuoka University, Fukuoka 814-0180, Japan*
[5]*Division of Nephrology and Kidney Center, Kobe University Graduate School of Medicine, Kobe 650-0017, Japan*
[6]*Department of Pathology, Faculty of Medicine, Fukuoka University, Fukuoka 814-0180, Japan*
[7]*Tokyo Kidney Research Institute, Tokyo 113-0023, Japan*
[8]*First Department of Internal Medicine, Sapporo Medical University School of Medicine, Sapporo 060-8543, Japan*
[9]*Department of Hematology and Immunology, Kanazawa Medical University, Kanazawa 920-0293, Ishikawa, Japan*
[10]*Department of Internal Medicine, Nagaoka Red Cross Hospital, Nagaoka 940-2085, Japan*

Correspondence should be addressed to Mitsuhiro Kawano, sk33166@gmail.com

Received 30 November 2011; Accepted 11 June 2012

Academic Editor: Vikram Deshpande

Although tubulointerstitial nephritis with IgG4+ plasma cell (PC) infiltration is a hallmark of IgG4-related kidney disease (IgG4-RKD), only a few studies are available about the minimum number of IgG4+ PC needed for diagnosis along with IgG4+/IgG+ PC ratio in the kidney. In addition, the significance of the deposition of IgG or complement as a reflection of humoral immunity involvement is still uncertain. In this study, we analyzed 20 Japanese patients with IgG4-RKD to evaluate the number of IgG4+ PCs along with IgG4+/IgG+ PC ratio and involvement of humoral immunity. The average number of IgG4+ PCs was 43.8/hpf and the average IgG4+/IgG+ or IgG4+/CD138+ ratio was 53%. IgG and C3 granular deposits on the tubular basement membrane (TBM) were detected by immunofluorescence microscopy in 13% and 47% of patients, respectively. Nine patients had a variety of glomerular lesions, and 7 of them had immunoglobulin or complement deposition in the glomerulus. In conclusion, we confirmed that infiltrating IgG4+ PCs > 10/hpf and/or IgG4/IgG (CD138)+ PCs > 40% was appropriate as an item of the diagnostic criteria for IgG4-RKD. A relatively high frequency of diverse glomerular lesions with immunoglobulin or complement deposits and deposits in TBM may be evidence of immune complex involvement in IgG4-related disease.

1. Introduction

The main histopathological finding in the kidney of IgG4-RD is tubulointerstitial nephritis (TIN) [1–3], which may result in renal failure [4]. IgG4-related TIN is composed of dense lymphoplasmacytic infiltrates with fibrosis and copious IgG4+ plasma cell infiltration, which are common features shared by other involved organs [5], and these

common pathologic features in the kidney have clearly been described by previous studies [1–3]. However, the minimum number of IgG4+ plasma cells needed for diagnosis has been differently reported in each affected organ [6–9], and only a few studies are available about the actual number of IgG4+ plasma cells evaluated along with IgG4+/IgG+ plasma cell ratio in IgG4-related kidney disease (IgG4-RKD) [2].

In addition to this issue, case reports or case series of a variety of glomerular disease concurrent with TIN have been accumulated [10–26]. These glomerular lesions are frequently accompanied by immunoglobulin or complement deposits suggesting that immune complexes might be involved in the pathogenesis of some cases with IgG4-RKD [2, 3]. However, the significance of these glomerular lesions as a reflection of humoral immunity involvement is still uncertain, and whether these glomerular lesions represent some IgG4-related kidney lesions with common etiopathological background or unrelated lesions merely concurrent with IgG4-TIN is still controversial.

In this study, we analyzed 20 Japanese patients with IgG4-RKD that were collected in our previous study aimed at establishing diagnostic criteria for IgG4-RKD [27], to address these pathological issues about the number of IgG4+ plasma cells along with IgG4+/IgG+ plasma cell ratio and involvement of humoral immunity in Japanese IgG4-RKD patients.

2. Methods

2.1. Patients. Between 2004 and 2011, we found 41 patients with IgG4-RKD in Kanazawa University Hospital, Nagaoka Red Cross Hospital, Niigata University Hospital, Sapporo Medical University Hospital, and Fukuoka University Hospital, of whom 28 underwent renal biopsy. In the remaining 13 patients with IgG4-RKD without renal biopsy, 4 had only pelvic lesion and 9 had typical radiologic findings such as multiple low-density lesions on enhanced CT, high serum IgG4 levels, and other organ involvement with biopsy proven IgG4+ plasma cell infiltration. In addition, these 9 patients had radiographic improvement after successful corticosteroid treatment. Of these 28 patients, 20 who received renal needle biopsy were included in this study because they had sufficient data to determine the number of IgG4-positive cells, IgG4/IgG or IgG4/CD138 ratio, and immunofluorescence microscopy or electron microscopy. Five patients with glomerular lesions (2 Henoch-Schönlein purpura [28, 29]; 2 membranous glomerulonephritis [4, 30]; 1 membranoproliferative glomerulonephritis [23]) were reported as case reports previously. Ten patients with crescentic glomerulonephritis or antineutrophil cytoplasmic antibodies (ANCA) associated vasculitis (1 Churg-Strauss syndrome; 1 Wegener's granulomatosis; 4 microscopic polyangiitis; 4 renal limited ANCA vasculitis) were also included in the study of infiltrating IgG4+ plasma cells as a control because IgG4+ plasma cell infiltration in some patients with ANCA associated vasculitis has been shown in previous studies [2, 31, 32]. Written informed consent for use of all data and samples was obtained from each patient. The diagnosis of IgG4-RKD was made based on the histopathologic findings of one or more organs, characteristic diagnostic imaging findings, elevated serum IgG4 levels, and other organ involvement typical for IgG4-RD. This study was approved by each institutional ethics board and the ethics board of the Japanese Society of Nephrology. The research was conducted in compliance with the Declaration of Helsinki.

2.2. Clinical Features. The clinical picture including allergic symptoms and those resulting from other organ involvement of IgG4-RD was noted. Serum IgG, IgG4, IgE, complement, and creatinine levels were obtained from the clinical data file. Urinary abnormalities including proteinuria, hematuria, and casturia were collected.

2.3. Imaging. Computed tomography (CT) with or without enhancement with contrast medium was performed before corticosteroid therapy to make the diagnosis of kidney involvement. Other modalities including gallium scintigraphy, magnetic resonance imaging, and fluorodeoxyglucose positron emission tomography were also employed to identify renal and extra-renal lesions.

2.4. Histology and Immunostaining. Bouin's fluid-fixed or formalin-fixed and paraffin-embedded renal specimens of patients with IgG4-RKD were analyzed, and tubulointerstitial nephritis with or without glomerular lesions was evaluated. These specimens were stained with hematoxylin and eosin (HE), periodic acid-Schiff (PAS), periodic acid methenamine silver (PAM), and Masson's trichrome for light microscopy (LM). Immunofluorescence microscopy was performed against IgG, IgA, IgM, C3, C1q, and fibrinogen. Immunostaining for infiltrating plasma cells was performed using mouse monoclonal antibody against human IgG4 (Zymed Laboratory, San Francisco, CA, USA, or The Binding Site, Birmingham, UK), antihuman IgG (Dako, Glostrup, Denmark), and/or antihuman CD138 (AbD serotec, Oxford, UK). IgG4+ plasma cells were counted in five different high power fields (hpf) (×400 magnification with an eyepiece with a field number of 22) with intensive infiltration, and the average IgG4+ plasma cell count was calculated. Average of IgG4+/IgG+ or IgG4+/CD138+ plasma cell ratio of at least two different hpf (2–5 hpf) was calculated.

2.5. Statistical Analysis. Mann-Whitney U test or Fisher's exact probability test was employed for the statistical analyses. A value of <0.05 was considered statistically significant.

3. Results

3.1. Clinical and Laboratory Features. The patients were 18 men and 2 women with an average age 64 years (range: 55 to 83). Table 1 shows clinical and laboratory features of the patients with IgG4-related TIN. Six patients had elevated serum creatinine levels (>2 mg/dL). The mean serum IgG level was 3479 mg/dL (range 1679–5380 mg/dL), and the mean serum IgG4 level was 923 mg/dL (range 408–1860 mg/dL) with all patients having elevated serum IgG4 levels. Hypocomplementemia was detected in 13 patients. Serum IgE level was evaluated in 11 of 12 patients tested.

Table 1: Clinical and laboratory features of IgG4-related tubulointerstitial nephritis.

Pt. no.	Age/gender	U-Prot	Cr	IgG	IgG4	IgE	CH50	C3	C4	Other organ involvement
1	76/F	—	0.59	2,990	769	267	60	110	27	Sa, Lu
2	70/M	0.26 g/day	0.90	3,496	623	NA	<12	52	2	Pa
3	59/M	—	1.10	2,319	734	542	>66.0	106	24	Sa, Pa, Pr, RP
4	63/M	0.2 g/gCr	1.20	1,756	408	513	51	98	16	Sa, Pa, Lu, Ao
5	58/M	0.2 g/gCr	1.20	3,170	1,204	3,960	<10	33	7	Sa, LN, Lu
6	58/M	—	1.30	1,960	1,280	456	34	81	16	Li, Ne
7	75/M	0.21 g/day	1.34	5,380	587	NA	<14	41	<5	Sa, LN, Lu
8	68/M	0.1 g/day	1.37	2,995	670	2,323	10	41	2	Sa
9	75/M	0.22 g/day	2.34	1,679	890	631	52	81	29	Sa
10	55/M	0.5 g/day	2.10	5,040	1,780	NA	49	74	36	Sa, Pa
11	69/M	0.25 g/day	2.36	4,001	1,340	NA	10	55	2	Pa
12	80/M	0.4 g/day	1.60	4,657	660	NA	<12	35	<1	Pa
13	68/M	—	1.90	3,830	736	NA	3	33	1	Sa, LN
14	79/M	—	0.60	4,756	409	457	8	41	3	Jo
15	69/M	1.0 g/gCr	7.26	4,661	1,120	335	5	10	7	La, Sa, LN, Pa, Lu, Pr
16	72/M	0.22 g/day	0.80	4,359	1,100	537	<12	55	3	LN
17	75/F	3.0 g/gCr	2.25	3,695	486	1,226	2	18	2	Sa, LN, Lu
18	83/M	2.3 g/day	1.48	3,144	944	32.1	16	56	6	—
19	60/M	0.5 g/gCr	1.59	1,952	886	575	56	86	21	La, Sa
20	78/M	1.4 g/day	6.17	3,731	1,860	NA	27.3	57	28	Pa

Note: Conversion factor for Cr: mg/dL to μmol/L, ×88.4.
Abbreviations: Ao: aorta; CH50, serum CH50 (U/mL); Cr: serum creatinine (mg/dL); C3: serum C3 (mg/dL); C4: serum C4 (mg/dL); IgG: serum immunoglobulin G (mg/dL); IgG4: serum immunoglobulin G4 (mg/dL); IgE: serum immunoglobulin E (IU/mL); Jo: joint; La: lacrimal gland; Li: liver; LN: lymph node; Lu: lung; NA: not available; Ne: nerve; Pa: pancreas; Pr: prostate; RP: retroperitoneum; Sa: salivary gland; U-Prot: proteinuria.

All patients except one had other organ involvement, and the clinical picture in relation to systemic organ involvement contributed to making the diagnosis of IgG4-RD. Frequently, involved organs were the salivary gland, pancreas, and lung. Twelve patients had sialadenitis, and 7 autoimmune pancreatitis type 1.

3.2. Histology and Immunostaining. Table 2 shows histologic features of 20 patients with IgG4-related TIN. Dense lymphoplasmacytic infiltration with fibrosis in the interstitium was a common feature, but one patient did not have obvious fibrosis. In immunohistochemistry, the average number of IgG4 positive plasma cells was 43.8/hpf (range 10–156/hpf), and average IgG4+/IgG+ or IgG4+/CD138+ ratio was 53% (range 18–90%). All patients fulfilled the histologic part of our diagnostic criteria for IgG4-related kidney disease, namely, infiltrating IgG4-positive plasma cells >10/hpf and/or IgG4/IgG (CD138)-positive plasma cells >40% [27]. IgG and C3 granular deposits on the tubular basement membrane (TBM) were detected by immunofluorescence microscopy in 2 (13%) and 7 (47%) of 15 patients for whom pathological reports about TBM staining were available. Granular C1q deposits on TBM were detected by IF in 2 (13%) of 15 patients. Of these, C3 granular deposits in the tubular basement membranes without accompanying IgG were thought to be a nonspecific feature because of possible production of C3 by tubular epithelial cells. Electron dense deposits were detected by electron microscopy (EM) in 6 (40%) of 15 patients. Glomerular lesions concurred with IgG4-related TIN in 9 patients, in all of whom other immune complex-mediated glomerulopathies such as lupus nephritis, Sjögren's syndrome, and cryoglobulinemia were ruled out by appropriate clinical, biochemical, serological, and other testing. The most frequently observed glomerular lesion was membranous glomerulonephritis, and three patients had this lesion (Figure 1). These patients did not have any mesangial or subendothelial dense deposits suggesting secondary membranous glomerulonephritis such as lupus nephritis. Similarly, they did not have clinical features suggesting secondary forms of membranous glomerulonephritis such as hepatitis B or C. Two patients had Henoch-Schönlein purpura nephritis (Figure 2) with typical purpuric skin lesions, the histopathology of which was composed of typical leukocytoclastic vasculitis with neutrophils and rare IgG4+ plasma cells. In addition, one patient showed IgA positive staining in the skin, while IgA immunostaining was not performed in the other patient. The remaining glomerular lesions were IgA nephropathy (Figure 3), membranoproliferative glomerulonephritis, and focal and segmental endocapillary hypercellularity.

3.3. Comparison between IgG4-Related TIN with and without Glomerular Lesions. Table 3 shows a comparison between IgG4-related TIN with or without glomerular lesions. The mean age of the glomerular lesion positive group (GL group) was higher than that of the glomerular lesion negative group (nonGL group) (73.8 ± 7.2 versus 66.0 ± 7.7 y; $P < 0.05$). Serum C3 levels of the GL group tended to be lower than

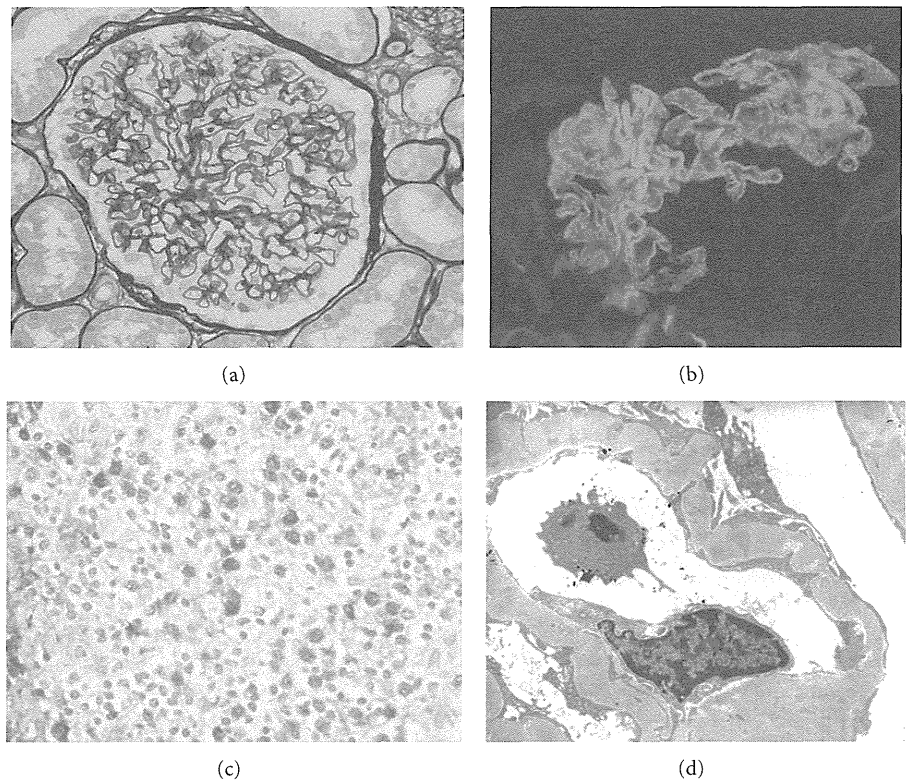

FIGURE 1: IgG4-related tubulointerstitial nephritis with membranous glomerulonephritis. (a) Periodic acid methenamine silver (PAM) staining reveals spike and bubbling formation (PAM ×400). (b) Immunofluorescence staining for IgG reveals granular deposits along the glomerular capillary walls (×400). (c) Many IgG4+ plasma cells are seen in the interstitium (IgG4 ×400). (d) Electron microscopy (EM) shows subepithelial deposits and variable reabsorption of these deposits with thickened glomerular basement membrane. (Ehrenreich-Churg stage II–IV).

those of the nonGL group (43 ± 23 versus 70 ± 27), but the difference was not statistically significant. The average number of IgG4 positive plasma cells, average IgG4+/IgG+ or IgG4+/CD138+ ratio, frequency of IgG, C3, C1q, and electron dense deposits on the TBM were not significantly different between the two groups.

3.4. IgG4-Positive Plasma-Cell-Rich ANCA-Associated Vasculitis. We analyzed 10 patients with ANCA-associated vasculitis immunohistochemically. Of these, 6 patients had more than 30/hpf plasma cell infiltration in the interstitium. Using IgG4 immunostaining, we found four patients with ANCA-associated vasculitis who fulfilled the immunohistochemical item of the diagnostic criteria of IgG4-related kidney disease (Figures 4(a) and 4(b)). Table 4 shows a summary of these four patients, all of whom had infiltrating IgG4-positive plasma cells >10/hpf and IgG4/CD138-positive plasma cells >40%. In contrast, in 2 patients only a small part of the infiltrating plasma cells were IgG4 positive (Figures 4(c) and 4(d)).

4. Discussion

In this study, we showed data about IgG4 positive plasma cell number per high power field (hpf) and IgG4+/IgG+ or IgG4+/CD138+ plasma cell ratios in the kidneys in some Japanese patients with IgG4-RKD. In addition, we compared IgG4-RKD patients with glomerular lesions with those without them clinically.

The number of IgG4+ plasma cells varies in affected organs and according to the biopsy method used (percutaneous needle biopsy or open surgical biopsy) [6–9]. As the kidney is suited for percutaneous needle biopsy and this method is most commonly chosen, obtained samples are relatively small and insufficient material is obtained in some cases. Therefore, to choose the most appropriate cutoff level in IgG4-RKD, the accumulation of studies focused on the infiltrating number of IgG4+ cells in the kidneys is needed. Our result supported the previously proposed cutoff value of >10/hpf [2]. On the other hand, 15 of 20 patients fulfilled the criterion of IgG4+/IgG+ plasma cell ratio > 40%, while the remaining 5 patients showed a ratio less than or equal to 40%. Thus, the quantitative assessment of infiltrating IgG4-positive plasma cells seems to supplement the IgG4+/IgG+ (CD138+) plasma cell ratio if this ratio is less than or equal to 40%.

Raissian et al. showed that 25 of 30 patients (83%) had TBM immune complex deposits by immunofluorescence microscopy (IF) or electron microscopy (EM) [2]. In contrast, we found that 47% of patients had C3 deposits in TBM

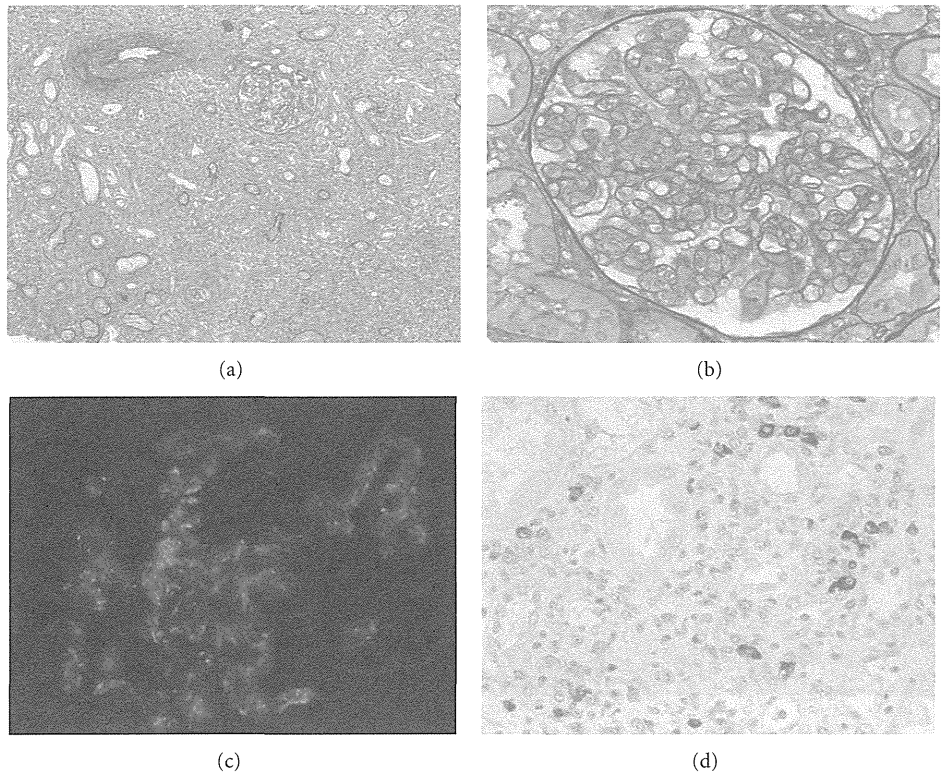

FIGURE 2: IgG4-related tubulointerstitial nephritis with Henoch-Schönlein purpura nephritis. (a) Periodic acid-Schiff (PAS) staining reveals severe tubulointerstitial nephritis (PAS ×100). (b) Global endocapillary proliferation is evident (PAS ×400). (c) Immunofluorescence staining for C3 reveals mesangial and capillary wall deposits (×400). (d) Many IgG4+ plasma cells are seen in the interstitium (IgG4 ×400).

TABLE 2: Histologic features of IgG4-related tubulointerstitial nephritis.

Pt. no.	Age/gender	IgG4 IHC (cells per hpf)	IgG4/IgG	Glomerular Lesion	IF TBM IgG	IF TBM C3	IF TBM C1q	IF GL IgG	IF GL IgA	IF GL C3	IF GL C1q	EM TBM	EM GL
1	76/F	50	81%	–	–	+	–	–	–	–	–	–	–
2	70/M	19	38%	–	NA	NA	NA	NA	NA	NA	NA	+	–
3	59/M	57	54%	–	–	–	–	–	–	–	–	NA	–
4	63/M	37	46%	–	–	+	+	–	–	–	–	–	–
5	58/M	21	81%	–	NA	NA	NA	–	–	–	NA	NA	–
6	58/M	156	77%	–	–	–	–	–	–	–	–	–	–
7	75/M	25	18%	–	–	–	–	NA	NA	NA	NA	+	–
8	68/M	17	40%	–	–	–	–	+	–	+	–	–	–
9	75/M	28	64%	–	+	+	–	–	–	–	–	±	–
10	55/M	49	55%	–	–	–	–	±	–	–	–	–	–
11	69/M	30	51%	–	–	–	–	+	–	–	2+	+	–
12	80/M	10	90%	MPGN	NA	NA	NA	2+	–	2+	+	NA	+
13	68/M	28	38%	IgA GN	–	+	–	–	2+	±	±	NA	NA
14	79/M	42	41%	EC	–	+	+	–	–	–	–	+	–
15	69/M	73	57%	EC	–	–	–	–	–	+	–	–	–
16	72/M	51	58%	HSPN	NA	NA	NA	2+	+	±	–	NA	+
17	75/F	62	40%	HSPN	–	–	–	–	+	2+	–	–	+
18	83/M	25	43%	MGN	+	+	–	+	–	+	–	+	+
19	60/M	68	42%	MGN	–	–	–	3+	–	–	–	–	+
20	78/M	28	45%	MGN	–	+	–	–	–	–	–	–	+

Abbreviations: EC: endocapillary hypercellularity; EM: electron microscopy; GL: glomeruli; hpf: high-power field; HSPN: Henoch-Schönlein purpura nephritis; IF: immunofluorescence; IgA GN: IgA nephropathy; IHC: immunohistochemistry; MGN: membranous glomerulonephritis; MPGN: membranoproliferative glomerulonephritis; NA: not available; Pt.: patient; TBM: tubular basement membranes.

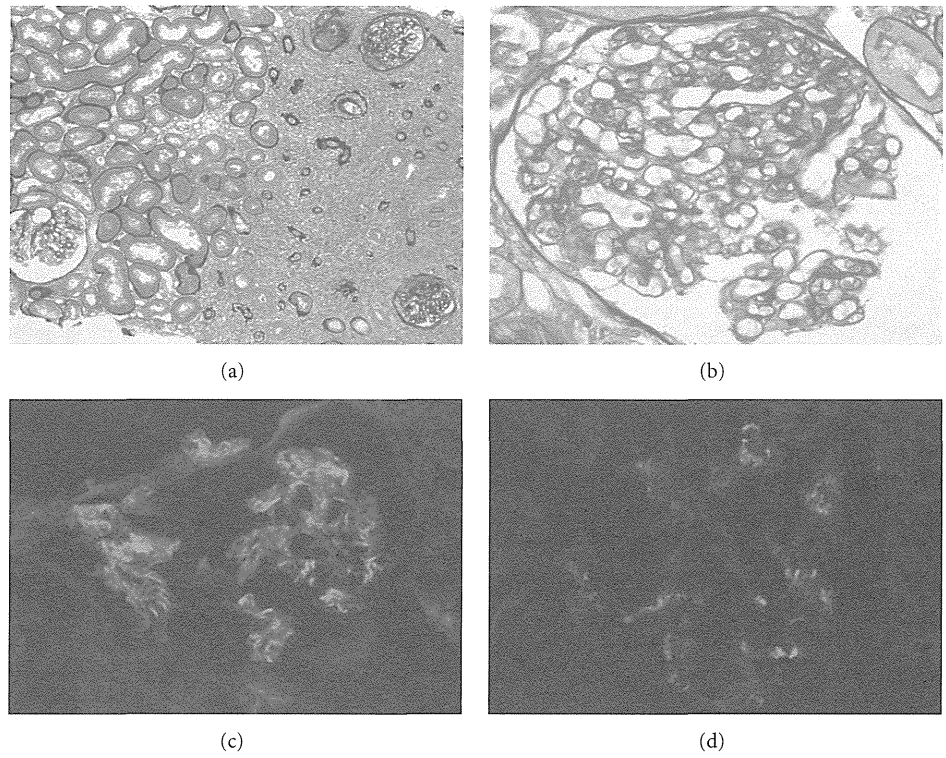

FIGURE 3: IgG4-related tubulointerstitial nephritis with IgA nephropathy. (a) Periodic acid-Schiff (PAS) staining reveals severe tubulointerstitial nephritis (PAS x100). Regional lesion distribution is evident. (b) Segmental mesangial proliferation is seen (PAS ×400). (c) Immunofluorescence staining for IgA reveals bright mesangial deposits (×400). (d) Immunofluorescence staining for C3 reveals weak mesangial staining for C3 (×400).

TABLE 3: Laboratory difference between IgG4-TIN patients with glomerular lesions and those without glomerular lesions.

	IgG4-TIN with GL	IgG4-TIN without GL	*P* value
Number of patients	9	11	
Age (years), mean ± SD	73.8 ± 7.2	66.0 ± 7.7	0.036
Serum creatinine (mg/dL)	2.6 ± 2.4	1.4 ± 0.6	0.239
Serum IgG (mg/dL)	3865 ± 903	3162 ± 1251	0.16
Serum IgG4 (mg/dL)	909 ± 434	935 ± 413	0.909
SerumC3 (mg/dL)	43 ± 23	70 ± 27	0.068
Low C4	7/9	5/11	0.197
Low CH50	7/9	5/11	0.197
IgG4 IHC (cells per hpf)	43.0 ± 21.8	44.5 ± 39.4	0.493
IgG4/IgG (%)	50.4 ± 16.5	54.1 ± 20.8	0.518
IF TBM IgG	1/7	1/9	>0.999
IF TBM C3	4/7	3/9	0.615
IF TBM C1q	1/7	1/9	>0.999
EM TBM	2/6	4/9	>0.999

Note: Conversion factor for creatinine: mg/dL to μmol/L, ×88.4.
Abbreviations: EM: electron microscopy; GL: glomerular lesions; hpf: high-power field; IF: immunofluorescence; IHC: immunohistochemistry; TBM: tubular basement membranes; TIN: tubulointerstitial nephritis.

TABLE 4: IgG4-positive plasma-cell-rich ANCA-related vasculitis.

Pt. no.	Age/gender	Diagnosis	PC infiltration	IgG4/hpf	IgG4/CD138 ratio (%)
1	75/F	CSS	++	19	47
2	59/M	mPA	++	22	52
3	79/F	mPA	+++	34	78
4	67/F	RLV	++	19	69

Abbreviations: CSS: Churg-Strauss syndrome; hpf: high-power field; mPA: microscopic polyangiitis; PC: plasma cell; RLV: renal limited vasculitis.

by IF and 13% of them had IgG deposits in TBM by IF. The difference in the frequency of TBM deposits might be due to a population difference, or IF sample size which might be smaller in our study. Although the frequency is different, the fact that more than 40% of patients were shown to have TBM deposits implies a close relationship between TBM deposits and IgG4-RKD. TBM deposits may thus show some immune complex involvement in IgG4-related disease.

Glomerular diseases sometimes concur with tubulointerstitial nephritis in patients with IgG4-related disease [4, 10, 12, 20, 23, 24, 28–30]. These include IgA nephropathy, Henoch-Schönlein purpura nephritis, endocapillary proliferative nephritis, crescentic glomerulonephritis, and membranous glomerulonephritis (MGN). Of these, MGN is

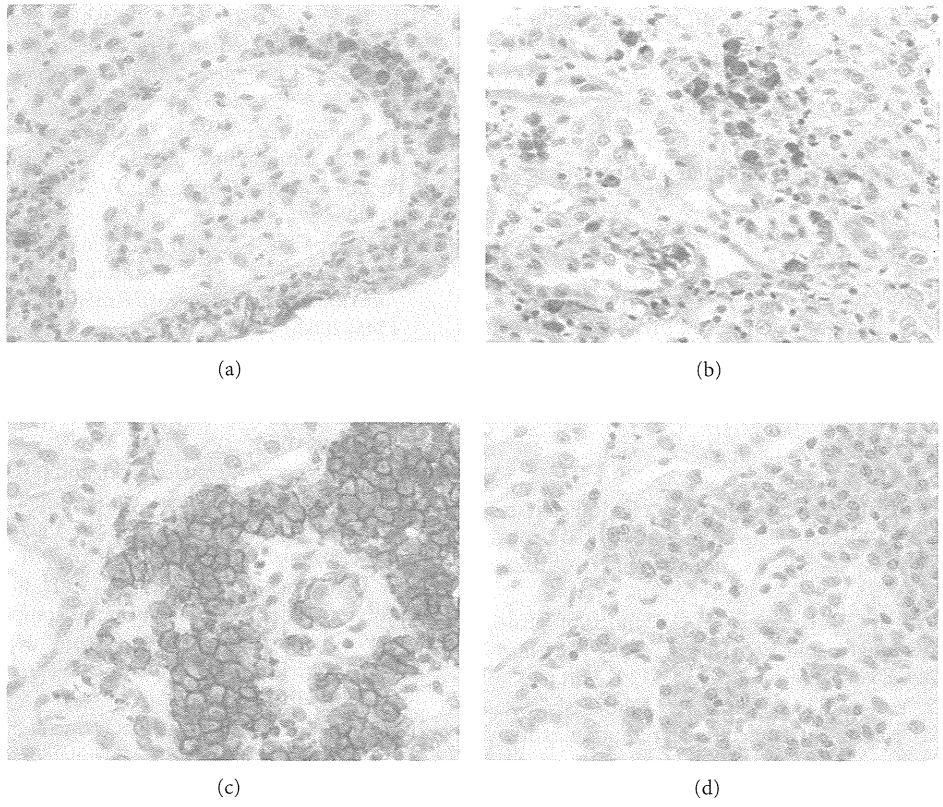

FIGURE 4: Anti-neutrophil cytoplasmic antibodies (ANCA) associated vasculitis. (a) IgG4+ plasma cells surround a glomerulus (IgG4 immunostaining ×400). (b) Accumulation of many IgG4+ plasma cells is seen in the interstitium (IgG4 immunostaining ×400). (c) Many CD138+ cells are seen in the interstitium (CD138 immunostaining ×400). (d) These plasma cells are IgG4 negative (IgG4 immunostaining x400).

the most frequently reported glomerular pathology [10, 12, 30, 33–35].

Interestingly, the first IgG4-RKD case reported by Uchiyama-Tanaka et al. had tubulointerstitial nephritis with MGN, and subepithelial and intramembranous electron-dense deposits disappeared after successful corticosteroid therapy [10]. In contrast, Watson et al. reported a second patient with IgG4-related TIN with MGN, the steroid responsiveness of which differed markedly and whose proteinuria persisted despite 7-months treatment [12]. Although laboratory and immunohistochemical features were not significantly different between IgG4-related TIN with or without glomerular lesions in this study, further studies will be necessary including some focused on the responsiveness to treatment.

MGN detected during the clinical course of IgG4-RD is classified into two groups based on the presence or absence of simultaneous overlapping of TIN. Cravedi et al. reported a patient with IgG4-RD of the pancreas with salivary gland involvement who developed proteinuria after the cessation of successful steroid therapy [34]. The renal biopsy revealed pure MGN without IgG4+ plasma cell rich TIN. Palmisano et al. also reported a pure MGN development in a patient with IgG4-related chronic periaortitis [35]. These two cases had in common MGN development without IgG4+ plasma cell infiltration in the clinical course of typical IgG4-RD. Although these cases seem to be pure MGN, careful judgment is needed because regional lesion distribution is a feature of IgG4-TIN, and sometimes only unaffected samples are obtained by percutaneous needle biopsy.

Although case reports of Henoch-Schönlein purpura (HSP) nephritis associated with IgG4-RD are very rare and only our two cases are so far known [28, 29], occasional development of anaphylactoid purpura in patients with IgG4-RD has been experienced (personal communication). As involvement of an allergic background is commonly presumed in both diseases, we should carefully evaluate the association of HSP with IgG4-RD when IgG4-RD patients have purpura.

In conclusion, we confirmed that infiltrating IgG4-positive plasma cells >10/hpf and/or IgG4/IgG (CD138)-positive plasma cells >40% was appropriate as an item of the diagnostic criteria for IgG4-RKD. Relatively high frequency of a variety of glomerular lesions concurrent with characteristic IgG4+ plasma-cell-rich lymphoplasmacytic infiltration with fibrosis seemed to show evidence of immune complex involvement in IgG4-related disease. However, as the number of analyzed cases in this study is small and some bias exists in case selection, worldwide study is needed to clarify the accurate frequency of the glomerular lesions in IgG4-RKD

and pathophysiological significance of immune deposits in TBM and in the glomerular lesion.

Conflict of Interests

The authors declare that there is no conflict of interests.

Acknowledgments

This work was supported partially by a grant from the Research Program of Intractable Diseases provided by the Ministry of Health, Labor, and Welfare of Japan. We thank Mr. J. S. Gelblum for his critical reading of the manuscript.

References

[1] T. Saeki, S. Nishi, N. Imai et al., "Clinicopathological characteristics of patients with IgG4-related tubulointerstitial nephritis," *Kidney International*, vol. 78, no. 10, pp. 1016–1023, 2010.

[2] Y. Raissian, S. H. Nasr, C. P. Larsen et al., "Diagnosis of IgG4-related tubulointerstitial nephritis," *Journal of the American Society of Nephrology*, vol. 22, no. 7, pp. 1343–1352, 2011.

[3] Y. Yamaguchi, Y. Kanetsuna, K. Honda, N. Yamanaka, M. Kawano, and M. Nagata, "Characteristic tubulointerstitial nephritis in IgG4-related disease," *Human Pathology*, vol. 43, no. 4, pp. 536–549, 2012.

[4] Y. Saida, N. Homma, H. Hama et al., "A case of IgG4-related tubulointerstitial nephritis showing the progression of renal dysfunction after a cure for autoimmune pancreatitis," *Japanese Journal of Nephrology*, vol. 52, no. 1, pp. 73–79, 2010.

[5] Y. Zen and Y. Nakanuma, "IgG4-related disease: a cross-sectional study of 114 cases," *American Journal of Surgical Pathology*, vol. 34, no. 12, pp. 1812–1819, 2010.

[6] K. M. Lindstrom, J. B. Cousar, and M. B. S. Lopes, "IgG4-related meningeal disease: clinico-pathological features and proposal for diagnostic criteria," *Acta Neuropathologica*, vol. 120, no. 6, pp. 765–776, 2010.

[7] W. Cheuk, H. K. L. Yuen, and J. K. C. Chan, "Chronic sclerosing dacryoadenitis: part of the spectrum of IgG4-related sclerosing disease?" *American Journal of Surgical Pathology*, vol. 31, no. 4, pp. 643–645, 2007.

[8] S. T. Chari, T. C. Smyrk, M. J. Levy et al., "Diagnosis of autoimmune pancreatitis: the mayo clinic experience," *Clinical Gastroenterology and Hepatology*, vol. 4, no. 8, pp. 1010–1016, 2006.

[9] Y. Zen, M. Onodera, D. Inoue et al., "Retroperitoneal fibrosis: a clinicopathologic study with respect to immunoglobulin G4," *American Journal of Surgical Pathology*, vol. 33, no. 12, pp. 1833–1839, 2009.

[10] Y. Uchiyama-Tanaka, Y. Mori, T. Kimura et al., "Acute tubulointerstitial nephritis associated with autoimmune-related pancreatitis," *American Journal of Kidney Diseases*, vol. 43, no. 3, pp. e18–e25, 2004.

[11] S. I. Takeda, J. Haratake, T. Kasai, C. Takaeda, and E. Takazakura, "IgG4-associated idiopathic tubulointerstitial nephritis complicating autoimmune pancreatitis," *Nephrology Dialysis Transplantation*, vol. 19, no. 2, pp. 474–476, 2004.

[12] S. J. W. Watson, D. A. S. Jenkins, and C. O. S. Bellamy, "Nephropathy in IgG4-related systemic disease," *American Journal of Surgical Pathology*, vol. 30, no. 11, pp. 1472–1477, 2006.

[13] L. Rudmik, K. Trpkov, C. Nash et al., "Autoimmune pancreatitis associated with renal lesions mimicking metastatic tumours," *Canadian Medical Association Journal*, vol. 175, no. 4, pp. 367–369, 2006.

[14] H. Nakamura, H. Wada, T. Origuchi et al., "A case of IgG4-related autoimmune disease with multiple organ involvement," *Scandinavian Journal of Rheumatology*, vol. 35, no. 1, pp. 69–71, 2006.

[15] V. Deshpande, S. Chicano, D. Finkelberg et al., "Autoimmune pancreatitis: a systemic immune complex mediated disease," *American Journal of Surgical Pathology*, vol. 30, no. 2, pp. 1537–1545, 2006.

[16] K. Shimoyama, N. Ogawa, T. Sawaki et al., "A case of Mikulicz's disease complicated with interstitial nephritis successfully treated by high-dose corticosteroid," *Modern Rheumatology*, vol. 16, no. 3, pp. 176–182, 2006.

[17] M. Murashima, J. Tomaszewski, and J. D. Glickman, "Chronic tubulointerstitial nephritis presenting as multiple renal nodules and pancreatic insufficiency," *American Journal of Kidney Diseases*, vol. 49, no. 1, pp. e7–e10, 2007.

[18] L. D. Cornell, S. L. Chicano, V. Deshpande et al., "Pseudotumors due to IgG4 immune-complex tubulointerstitial nephritis associated with autoimmune pancreatocentric disease," *American Journal of Surgical Pathology*, vol. 31, no. 10, pp. 1586–1597, 2007.

[19] K. Yoneda, K. Murata, K. Katayama et al., "Tubulointerstitial nephritis associated with IgG4-related autoimmune disease," *American Journal of Kidney Diseases*, vol. 50, no. 3, pp. 455–462, 2007.

[20] K. Katano, Y. Hayatsu, T. Matsuda et al., "Endocapillary proliferative glomerulonephritis with crescent formation and concurrent tubulo-interstitial nephritis complicating retroperitoneal fibrosis with a high serum level of IgG4," *Clinical Nephrology*, vol. 68, no. 5, pp. 308–314, 2007.

[21] N. Mise, Y. Tomizawa, A. Fujii, Y. Yamaguchi, and T. Sugimoto, "A case of tubulointerstitial nephritis in IgG4-related systemic disease with markedly enlarged kidneys," *NDT Plus*, vol. 2, no. 3, pp. 233–235, 2009.

[22] A. Aoki, K. Sato, M. Itabashi et al., "A case of Mikulicz's disease complicated with severe interstitial nephritis associated with IgG4," *Clinical and Experimental Nephrology*, vol. 13, no. 4, pp. 367–372, 2009.

[23] J. Morimoto, Y. Hasegawa, H. Fukushima et al., "Membranoproliferative glomerulonephritis-like glomerular disease and concurrent tubulointerstitial nephritis complicating IgG4-related autoimmune pancreatitis," *Internal Medicine*, vol. 48, no. 3, pp. 157–162, 2009.

[24] I. Naitoh, T. Nakazawa, H. Ohara et al., "Autoimmune pancreatitis associated with various extrapancreatic lesions during a long-term clinical course successfully treated with azathioprine and corticosteroid maintenance therapy," *Internal Medicine*, vol. 48, no. 23, pp. 2003–2007, 2009.

[25] Y. Tsubata, F. Akiyama, T. Oya et al., "IgG4-related chronic tubulointerstitial nephritis without autoimmune pancreatitis and the time course of renal function," *Internal Medicine*, vol. 49, no. 15, pp. 1593–1598, 2010.

[26] F. Kim, K. Yamada, D. Inoue et al., "IgG4-related tubulointerstitial nephritis and hepatic inflammatory pseudotumor without hypocomplementemia," *Internal Medicine*, vol. 50, no. 11, pp. 1239–1244, 2011.

[27] M. Kawano, T. Saeki, H. Nakashima et al., "Proposal for diagnostic criteria for IgG4-related kidney disease," *Clinical and Experimental Nephrology*, vol. 15, no. 5, pp. 615–626, 2011.

[28] R. Tamai, Y. Hasegawa, S. Hisano et al., "A case of IgG4-related tubulointerstitial nephritis concurrent with Henoch-Schonlein purpura nephritis," *Allergy, Asthma and Clinical Immunology*, vol. 7, article 5, 2011.

[29] K. Ito, K. Yamada, I. Mizushima et al., "Henoch-Schönlein purpura nephritis in a patient with IgG4-related disease: a possible association ," *Clinical Nephrology*. In press.

[30] T. Saeki, N. Imai, T. Ito, H. Yamazaki, and S. Nishi, "Membranous nephropathy associated with IgG4-related systemic disease and without autoimmune pancreatitis," *Clinical Nephrology*, vol. 71, no. 2, pp. 173–178, 2009.

[31] M. Yamamoto, H. Takahashi, C. Suzuki et al., "Analysis of serum IgG subclasses in churg-strauss syndrome—the meaning of elevated serum levels of IgG4," *Internal Medicine*, vol. 49, no. 14, pp. 1365–1370, 2010.

[32] D. C. Houghton and M. L. Troxell, "An abundance of IgG4+ plasma cells is not specific for IgG4-related tubulointerstitial nephritis," *Modern Pathology*, vol. 24, no. 11, pp. 1480–1487, 2011.

[33] F. C. Fervenza, G. Downer, L. H. Beck Jr., and S. Sethi, "IgG4-related tubulointerstitial nephritis with membranous nephropathy," *American Journal of Kidney Diseases*, vol. 58, no. 2, pp. 320–324, 2011.

[34] P. Cravedi, M. Abbate, E. Gagliardini et al., "Membranous nephropathy associated with IgG4-related disease," *American Journal of Kidney Diseases*, vol. 58, no. 2, pp. 272–275, 2011.

[35] A. Palmisano, D. Corradi, M. L. Carnevali et al., "Chronic periaortitis associated with membranous nephropathy: clues to common pathogenetic mechanisms," *Clinical Nephrology*, vol. 74, no. 6, pp. 485–490, 2010.

Exacerbation of diabetic nephropathy by hyperlipidaemia is mediated by Toll-like receptor 4 in mice

T. Kuwabara, K. Mori, M. Mukoyama, M. Kasahara, H. Yokoi, Y. Saito, Y. Ogawa, H. Imamaki, T. Kawanishi, A. Ishii, K. Koga, K. P. Mori, et al.

Diabetologia
Clinical and Experimental Diabetes and Metabolism

ISSN 0012-186X
Volume 55
Number 8

Diabetologia (2012) 55:2256-2266
DOI 10.1007/s00125-012-2578-1

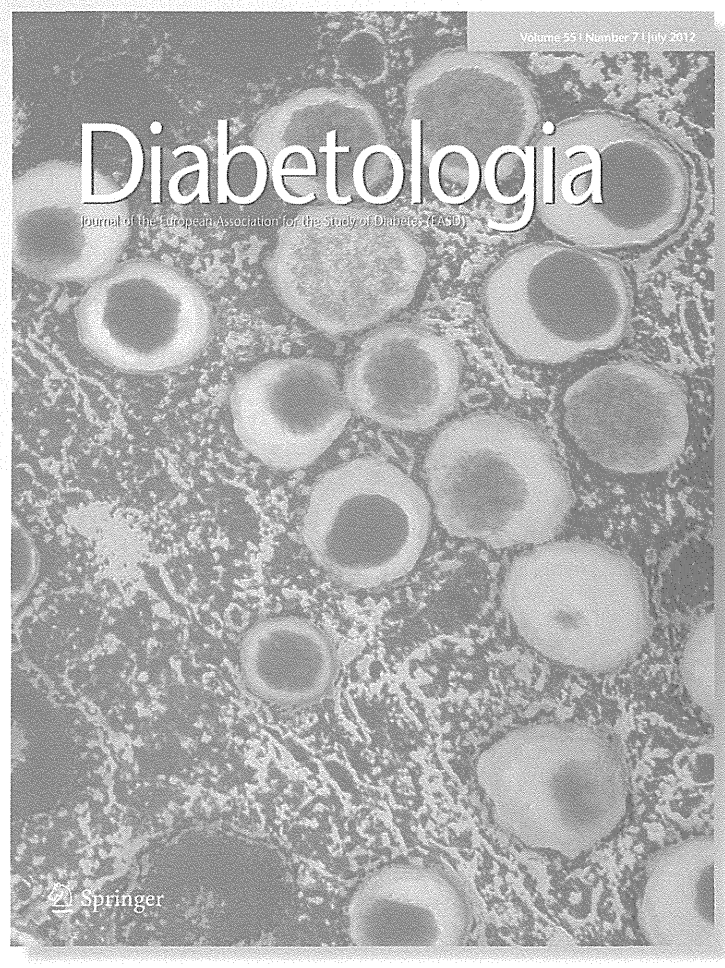

Springer

Diabetologia (2012) 55:2256–2266
DOI 10.1007/s00125-012-2578-1

ARTICLE

Exacerbation of diabetic nephropathy by hyperlipidaemia is mediated by Toll-like receptor 4 in mice

T. Kuwabara · K. Mori · M. Mukoyama · M. Kasahara · H. Yokoi · Y. Saito · Y. Ogawa · H. Imamaki · T. Kawanishi · A. Ishii · K. Koga · K. P. Mori · Y. Kato · A. Sugawara · K. Nakao

Received: 3 February 2012 / Accepted: 4 April 2012 / Published online: 19 May 2012

Abstract
Aims/hypothesis Hyperlipidaemia is an independent risk factor for the progression of diabetic nephropathy, but its molecular mechanism remains elusive. We investigated in mice how diabetes and hyperlipidaemia cause renal lesions separately and in combination, and the involvement of Toll-like receptor 4 (TLR4) in the process.
Methods Diabetes was induced in wild-type (WT) and *Tlr4* knockout (KO) mice by intraperitoneal injection of streptozotocin (STZ). At 2 weeks after STZ injection, normal diet was substituted with a high-fat diet (HFD). Functional and histological analyses were carried out 6 weeks later.
Results Compared with treatment with STZ or HFD alone, treatment of WT mice with both STZ and HFD markedly aggravated nephropathy, as indicated by an increase in albuminuria, mesangial expansion, infiltration of macrophages and upregulation of pro-inflammatory and extracellular-matrix-associated gene expression in glomeruli. In *Tlr4* KO mice, the addition of an HFD to STZ had almost no effects on the variables measured. Production of protein S100 calcium binding protein A8 (calgranulin A; S100A8), a potent ligand for TLR4, was observed in abundance in macrophages infiltrating STZ-HFD WT glomeruli and in glomeruli of diabetic nephropathy patients. High-glucose and fatty acid treatment synergistically upregulated *S100a8* gene expression in macrophages from WT mice, but not from KO mice. As putative downstream targets of TLR4, phosphorylation of interferon regulatory factor 3 (IRF3) was enhanced in kidneys of WT mice co-treated with STZ and HFD.
Conclusions/interpretation Activation of S100A8/TLR4 signalling was elucidated in an animal model of diabetic glomerular injury accompanied with hyperlipidaemia, which may provide novel therapeutic targets in progressive diabetic nephropathy.

Keywords Diabetic nephropathy · Glomerulus · High-fat diet · Hyperlipidaemia · Macrophages · S100A8 · TLR4

Abbreviations

BMDMs	Bone marrow-derived macrophages
C_t	Cycle threshold
CTGF	Connective tissue growth factor
ECM	Extracellular matrix
ESRD	End-stage renal disease
GAPDH	Glyceraldehyde-3-phosphate dehydrogenase
HFD	High-fat diet
IKB	Inhibitor κB
IRF3	Interferon regulatory factor 3
JNK	c-Jun N-terminal kinase
KO	Knockout
MAC-2	Lectin galactoside-binding, soluble, 3
MYD88	Myeloid differentiation primary response gene (88)
ND	Normal diet
nSTZ	non-STZ
PAS	periodic acid–Schiff

Electronic supplementary material The online version of this article (doi:10.1007/s00125-012-2578-1) contains peer-reviewed but unedited supplementary material, which is available to authorised users.

T. Kuwabara · K. Mori (✉) · M. Mukoyama · M. Kasahara · H. Yokoi · Y. Saito · H. Imamaki · T. Kawanishi · A. Ishii · K. Koga · K. P. Mori · Y. Kato · K. Nakao
Department of Medicine and Clinical Science,
Kyoto University Graduate School of Medicine,
54 Shogoin Kawaharacho, Sakyoku,
Kyoto 606-8507, Japan
e-mail: keyem@kuhp.kyoto-u.ac.jp

Y. Ogawa · A. Sugawara
Department of Nephrology, Osaka Redcross Hospital,
Osaka, Japan

S100A8	S100 calcium binding protein A8
S100A9	S100 calcium binding protein A9
STZ	Streptozotocin
TLR	Toll-like receptor
TRIF	TIR-domain-containing adapter-inducing interferon-β
WT	Wild-type

Introduction

Diabetic nephropathy is one of the most prevalent causes of end-stage renal disease (ESRD) [1]. Despite progress in pharmacological strategies to control diabetes, hypertension and other metabolic abnormalities, the number of patients entering ESRD because of diabetic nephropathy remains extremely high, and the development of new classes of therapeutic reagents is eagerly anticipated [2]. During recent decades, the pathophysiology of diabetic nephropathy has become complex and serious because of coexisting lifestyle-related disorders, such as hyperlipidaemia, hypertension and obesity [3]. In fact, hyperlipidaemia is an independent risk factor for the progression of diabetic nephropathy in both type 1 and type 2 diabetes [4, 5], but the underlying molecular mechanism remains elusive [6].

Toll-like receptors (TLRs) are a family of receptors that play a critical role in the innate immune system by activating pro-inflammatory signalling pathways in response to molecular patterns synthesised by microorganisms [7]. TLR4, one of the best-characterised TLRs, binds with lipopolysaccharide from Gram-negative bacterial cell walls and with several endogenous ligands [7]. TLR4 also plays an important role in various kidney disorders, such as glomerulonephritis, renal ischaemia and diabetic tubular inflammation [8–13], but the role of TLR4 in diabetic glomerular injury and hyperlipidaemia-induced kidney damage remains largely unknown.

In the current study, TLR4 and its novel endogenous ligand S100 calcium binding protein A8 (S100A8) emerged as candidate molecules involved in the progression of diabetic nephropathy by our microarray analysis performed in two different types of diabetic mouse models. Furthermore, we examined the effects of high-fat diet (HFD) feeding on streptozotocin (STZ)-induced diabetes in *Tlr4* knockout (KO) and wild-type (WT) mice in order to elucidate the mechanism for the progression of diabetic nephropathy caused by hyperlipidaemia.

Methods

Experimental animals Male *Tlr4* KO [14] and WT mice with a C57BL/6 J genetic background were studied. To generate a mouse model of diabetes complicated by hyperlipidaemia, 8-week-old mice were intraperitoneally injected with STZ (100 mg/kg body weight in citrate buffer, pH 4.0; Sigma-Aldrich, St Louis, MO, USA) or vehicle for 3 consecutive days. After 2 weeks, normal diet (ND; NMF, 14.7 kJ/g [3.5 kcal/g], 13% of energy as fat; Oriental Yeast, Tokyo, Japan) was substituted with an HFD (D12451, 19.7 kJ/g [4.7 kcal/g], 45% of energy as fat; Research Diets, New Brunswick, NJ, USA) in subgroups of animals, and all were killed for analysis at 8 weeks after STZ treatment. In another set of experiments, 8-week-old male *db/db* mice (on a BKS genetic background; Japan Clea, Tokyo, Japan) were randomly assigned to ND or HFD (D12492, 21.8 kJ/g [5.2 kcal/g], 60% of energy as fat; Research Diets) groups and followed for 4 weeks. All animal experiments were conducted in accordance with the Guidelines for Animal Research Committee of Kyoto University Graduate School of Medicine.

Human biopsy samples Human kidney samples obtained at renal biopsy carried out in our department were used for immunohistochemistry. The human study protocol was approved by the Ethical Committee on Human Research of Kyoto University Graduate School of Medicine. All participants gave written informed consent.

Measurement of metabolic variables Metabolic variables were measured as described previously [15, 16]. Briefly, blood pressure was measured by indirect tail-cuff method (Muromachi Kikai, Tokyo, Japan). Urine samples were collected with metabolism cages, and urinary albumin was measured with competitive ELISA (Exocell, Philadelphia, PA, USA). Serum and urinary creatinine levels were assayed by enzymatic method (SRL, Tokyo, Japan) [17]. Plasma glucose, triacylglycerol and total cholesterol levels were measured, under conditions of ad libitum feeding, using an enzymatic method (Wako Pure Chemicals, Osaka, Japan). Plasma insulin levels were measured by enzyme immunoassay (Morinaga, Tokyo, Japan). For measurement of tissue triacylglycerol content, lipids were extracted with isopropyl alcohol/heptane (1:1 [vol./vol.]) from frozen kidney samples. After evaporating the solvent, lipids were resuspended in 99.5% ethanol and triacylglycerol contents were measured as described above.

Real-time quantitative RT-PCR Total RNA was extracted with TRIzol reagent (Invitrogen, Carlsbad, CA, USA) and cDNA in each sample was synthesised using the High Capacity cDNA Reverse Transcription Kit (Applied Biosystems, Foster City, CA, USA) from mouse kidneys and glomeruli isolated by graded sieving method [18, 19]. TaqMan real-time PCR was performed using Premix Ex Taq (Takara Bio, Otsu, Japan) and StepOnePlus Real Time PCR System (Applied Biosystems, Foster City, CA, USA). See Electronic supplementary material (ESM) Table 1 for primer

and probe sequences. Expression levels of all genes were normalised by *Gapdh* (internal control) levels. The mean expression level in whole kidney of WT non-treated control mice was arbitrarily defined as 1.0.

Histological analysis Periodic acid–Schiff (PAS) staining of the mesangial area and immunohistochemistry of S100A8 (requiring antigen retrieval by citrate buffer) and lectin, galactoside-binding, soluble, 3 (MAC-2 or LGALS3) [18] were carried out using kidney sections (thickness 4 μm) fixed with 4% buffered paraformaldehyde. Nuclei were counterstained with haematoxylin. All the primary antibodies used in this study are shown in ESM Table 2. For double staining, primary antibody for S100A8 was visualised with DyLight-conjugated secondary antibody (Takara Bio, Otsu, Japan). Immunofluorescence of podocin (or NPHS2) was performed with snap-frozen cryostat sections (4 μm), pretreated with cold acetone and 0.1% Triton-X100, and with primary and FITC-labelled secondary antibodies. Photographs were taken by a fluorescence microscope (IX81-PAFM; Olympus, Tokyo, Japan). Mesangial and podocin-positive areas of more than ten glomeruli from the outer cortex were measured quantitatively to obtain an average for each mouse using MetaMorph 7.5 software (Molecular Devices, Downingtown, PA, USA). Formalin-fixed, snap-frozen sections (10 μm) were stained with Oil Red O to evaluate lipid-droplet-positive areas.

Microarray analysis Two different types of diabetic mouse model were employed for microarray analysis. Male A-ZIP/F-1 heterozygous transgenic mice and control male FVB/N littermates were used at 10 months of age, when A-ZIP/F-1 mice exhibited diabetic nephropathy with massive proteinuria [20]. The other model was STZ-induced, insulin-dependent, diabetic C57BL/6 J male mice (Japan Clea) in which diabetes was induced at 9 weeks of age by single intraperitoneal injection of STZ (180 mg/kg); mice were analysed 8 weeks later. We essentially followed the procedures described in detail in the GeneChip Eukaryotic Target Preparation & Hybridization Manual (Affymetrix, Santa Clara, CA, USA). In brief, cDNA was synthesised and biotin-labelled cRNA was produced through in vitro transcription labelling Kit (Affymetrix). Fragmented cRNA was hybridised to GeneChip Mouse Genome 430 2.0 Array (Affymetrix) at 45°C for 16 h. The samples were washed and stained according to the manufacturer's protocol on GeneChip Fludisc Station 450 (Affymetrix) and scanned on GeneChip Scanner 3000 (Affymetrix).

PCR array analysis To eliminate contaminating genomic DNA, total RNA extracted from kidney samples was purified using RNeasy Mini Kit (QIAGEN Sciences, Maryland, MD, USA). First-strand cDNA was synthesised from total RNA using the RT2 first-strand kit (SABiosciences, Frederick, MD, USA). The mouse TLR-signalling pathway RT2 Profiler PCR plate (PAMM-018, SABiosciences) and StepOnePlus were used for amplification of cDNA. The analysis used 96 well plates containing gene-specific primer sets for 84 relevant TLR pathway genes, five housekeeping genes and two negative controls. The cycle threshold (C_t) was determined for each sample and normalised to the average C_t of the five housekeeping genes. The comparative ΔC_t method (SABiosciences) was used to calculate relative gene expression.

Western blot analysis Proteins extracted from kidney samples were separated by SDS-PAGE, transferred onto PVDF membranes, incubated with primary antibodies and detected with peroxidase-conjugated secondary antibodies and chemiluminescence [19]. Glyceraldehyde-3-phosphate dehydrogenase (GAPDH) was used as an internal control.

Cultured macrophages Palmitate (Sigma-Aldrich) was solubilised in ethanol, and combined with fatty-acid-free, low endotoxin, bovine serum albumin (Sigma-Aldrich) at a molar ratio of 10:1 in serum-free medium. Polymyxin B (10 μg/ml, Nacalai Tesque, Kyoto, Japan) was added to each well to minimise contamination of endotoxin. Bone marrow-derived macrophages (BMDMs) were generated from mice as described previously [21]. Briefly, following lysis of erythrocytes, bone marrow cells were resuspended in medium containing 20% fetal calf serum and 50 ng/ml recombinant human macrophage colony-stimulating factor, and cultured at 37°C in 5% CO_2 atmosphere. On day 6, the medium was replaced with fresh medium containing 5.6 mmol/l or 25 mmol/l glucose. On day 7, macrophages were incubated with palmitate or vehicle for 24 h. Total RNA from cells was extracted with RNeasy Mini Kit, and mRNA expression levels of *S100a8* and *Tlr4* were determined by TaqMan real-time RT-PCR.

Statistical analysis Data are expressed as means±SEM. Differences between multiple groups were assessed by two-way factorial ANOVA with Bonferroni's post test. Comparisons between two groups were carried out by unpaired Student's *t* test. Statistical significance was defined as $p<0.05$.

Results

Changes of metabolic variables and albuminuria in WT diabetic mice given a fat-rich diet Metabolic variables of non-STZ (nSTZ)-HFD, STZ-ND, STZ-HFD and control nSTZ-ND groups of WT mice are shown in Table 1. HFD treatment (compared with ND) in nSTZ mice caused significant elevation of body weight, plasma glucose, insulin,

Table 1 Metabolic data of WT and *Tlr4* KO mice at 8 weeks after STZ injection

Variable	WT				KO			
	nSTZ-ND	nSTZ-HFD	STZ-ND	STZ-HFD	nSTZ-ND	nSTZ-HFD	STZ-ND	STZ-HFD
Number of animals	6	4	8	11	4	4	5	8
Body weight (g)	27.7±1.0	33.7±0.5**	20.0±0.9**	22.1±0.5**,§§§	34.9±2.4†	39.6±1.4†	22.0±1.3**	23.3±0.6***,§§§
Blood pressure (mmHg)								
Systolic	101±2	104±2	98±1	100±1	103±2	103±2	96±1*	101±2
Diastolic	56±2	57±3	52±2	56±2	55±1	57±2	50±1*	53±1
Kidney weight (% body weight)	0.5±0.0	1.0±0.0**	1.7±0.1**	1.8±0.1**,§§§	1.0±0.1†††	2.2±0.2***,††	1.9±0.2***	1.9±0.1***
Plasma glucose (mmol/l)	9.5±1.6	14.0±0.4*	40.0±3.9**	32.9±1.8**,§	10.4±1.1	12.7±2.3	36.0±7.7*	31.8±2.3***,§§
HbA_{1c} (%)	3.4±0.1	5.3±0.1**	9.6±0.6**	9.9±0.5**,§	3.0±0.3	4.9±0.2**	9.4±1.1**	10.3±0.3***,§§§
HbA_{1c} (mmol/mol)	13.3±1.4	34.1±0.7**	81.8±6.5**	84.6±5.1**,§	9.0±2.8	29.5±2.5**	78.9±12.5**	89.4±3.2***,§§§
Plasma insulin (pmol/l)	133±16	256±21**	10±2**	12±2**,§§§	238±43	336±33	12±5**	12±5**,§§§
Plasma triacylglycerol (mmol/l)	0.99±0.02	1.20±0.03**	2.36±1.01*	5.48±1.56*,§	1.74±0.32	1.42±0.11	3.12±1.56	7.64±1.58**,§§
Plasma total cholesterol (mmol/l)	1.5±0.4	3.4±0.3*	5.1±0.8*	5.2±0.5**	1.9±0.4	3.4±0.2*	3.8±0.6*	5.9±0.4**,§§,‡
Serum creatinine (μmol/l)	8.0±1.8	8.8±0.1	10.6±0.9	15.9±5.3	8.8±0.1	8.0±0.1††	10.6±1.8	8.0±0.1

Data are means±SEM

Blood was collected with mice fed ad libitum

*$p<0.05$, **$p<0.01$, ***$p<0.001$ vs nSTZ-ND; †$p<0.05$, ††$p<0.01$, †††$p<0.001$ vs similarly treated group of WT; ‡$p<0.05$ vs STZ-ND; §$p<0.05$, §§$p<0.01$, §§§$p<0.001$ vs nSTZ-HFD

triacylglycerol and total cholesterol levels. STZ treatment (compared with nSTZ) in ND mice caused significant body weight loss and significant elevation of plasma glucose, triacylglycerol and total cholesterol levels. Treatment of STZ mice with HFD resulted in large exacerbation of hypertriacylglycerolaemia (by 2.3-fold) without significant changes in other above-mentioned variables (Table 1). Consistently, renal lipid deposition in STZ-HFD mice was markedly increased compared with STZ-ND mice (Fig. 1a, b). Blood pressures were not significantly different among the four treatment groups (Table 1).

Concerning albuminuria, one of the representative abnormalities that characterise diabetic nephropathy [2], albumin excretion in STZ-ND was elevated by 2.3-fold at 8 weeks compared with nSTZ-ND mice (Fig. 1c). The addition of HFD to STZ mice further enhanced albuminuria approximately twofold. To investigate podocyte injury, we investigated whether podocin protein production is decreased in the glomeruli of STZ-HFD mice [19]. Glomerular podocin level was significantly reduced in STZ-ND compared with nSTZ-ND and was lowest in STZ-HFD (Fig. 1e, f). Also, in obese, type 2 diabetic *db/db* mice, albuminuria was exaggerated by HFD (ESM Fig. 1). To summarise, treatment of WT mice with a combination of HFD and STZ resulted in marked enhancement of hypertriglycerolaemia, renal lipid deposition, podocyte damage and albumin excretion.

Gene expression analysis of pro-inflammatory and extracellular-matrix-associated genes in whole kidney and glomeruli and histological examination We measured mRNA levels of pro-inflammatory and extracellular matrix (ECM)-associated genes both in whole kidney and isolated glomeruli (Fig. 2, ESM Table 3). The former set of genes included *Mcp1* (also known as *Ccl2*, encoding monocyte chemoattractant protein-1 [MCP1]), *F4/80* (also known as *Emr1*), *Cd68*, *Tnfa* (also known as *Tnf* [encoding TNF]), *Pai1* (also known as *Serpine1* [encoding plasminogen activator inhibitor-1]) and *Il1b* (encoding IL1β). The latter set comprised *Tgfb1* (encoding TGFβ1), *Fn* (also known as *Fn1* [encoding fibronectin]), *Col4a3* (encoding type IV collagen alpha 3 chain), *Ctgf* (encoding connective tissue growth factor [CTGF]) and *Mmp2* (encoding matrix metalloproteinase 2). We found that expression levels of these genes in glomeruli and whole kidney were mildly elevated in WT STZ-ND compared with WT nSTZ-ND mice, in general (Fig. 2, ESM Table 3). Gene expression levels were further upregulated in WT STZ-HFD animals. Of note, differences between nSTZ-HFD and nSTZ-ND groups were

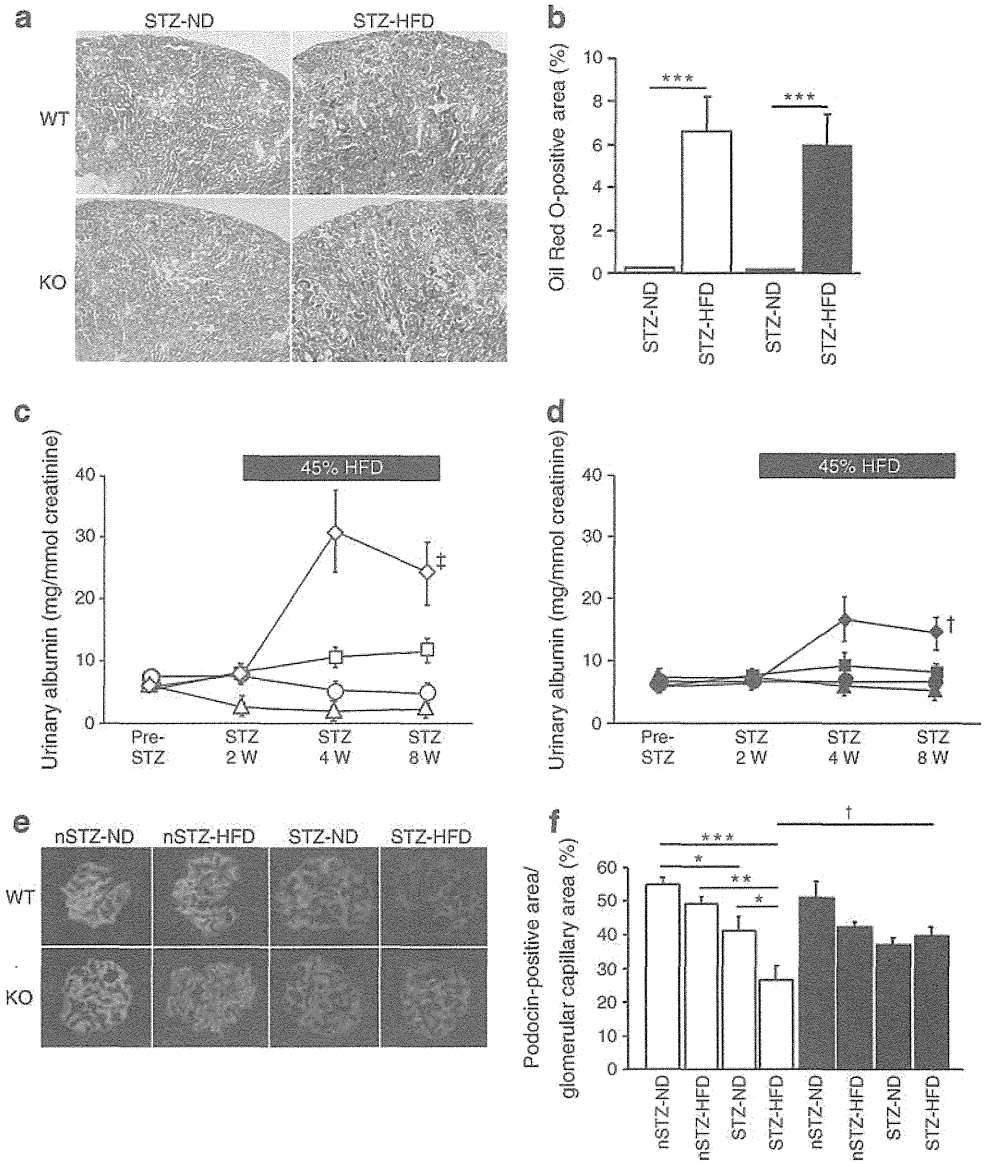

Fig. 1 Treatment of STZ diabetic mice with an HFD worsens renal injury in WT but not in *Tlr4* KO mice. (**a**, **b**) Addition of HFD to STZ mice causes similar degrees of deposition of lipid droplets staining positive with Oil Red O in WT (white bars) and KO mice (black bars) at 16 weeks of age. Magnification×4. Data are means±SEM. $n=5$. ***$p<0.001$. Time course of urinary albumin levels normalised with urinary creatinine levels in WT (**c**) and *Tlr4* KO mice (**d**). Circles, nSTZ-ND; triangles, nSTZ-HFD; squares, STZ-ND; diamonds, STZ-HFD. W, weeks after STZ injection. $n=6$–10. $^{‡}p<0.05$ vs WT STZ-ND, $^{†}p<0.05$ vs WT STZ-HFD calculated by area under the curve. (**e**, **f**) Immunofluorescence analysis of glomerular podocin level. White bars, WT; black bars, KO; $n=4$–6. *$p<0.05$, **$p<0.01$, ***$p<0.001$. $^{†}p<0.05$ for similarly treated KO vs WT

negligible (Fig. 2). Histological analysis also showed that MAC-2-positive-macrophage infiltration into glomeruli (Fig. 3a) and renal interstitium (ESM Fig. 2) and glomerular mesangial expansion (Fig. 3b) in STZ-HFD mice were markedly more pronounced than in STZ-ND mice.

Screening of candidate genes involved in the pathogenesis of diabetic nephropathy To identify candidate molecules potentially involved in the pathophysiology of diabetic nephropathy, we analysed gene expression profiles of diabetic mouse glomeruli by microarray (ESM Table 4). We compared two types of diabetic nephropathy from STZ-induced and A-ZIP/F-1 lipoatrophic diabetes mice. We selected commonly regulated genes to minimise interference from the renal toxicity of STZ, genetic background [22] and direct insulin or leptin target molecules [23]. The list of genes commonly upregulated in these two models included pro-inflammatory and ECM-associated genes and also ones encoding TLRs (ESM Table 4). As pairs of cell surface receptors and their ligands provide attractive seeds for future therapeutic targets, we focused on TLR4, for which glomerular levels were elevated by 1.7-fold by STZ and 5.8-fold in A-ZIP/F-1 compared with each control by microarray. We further examined the expression of genes encoding molecules reported to be endogenous ligands for TLR4 [7], and identified *S100a8* (also known as *Mrp8*) and *S100a9* (also known as *Mrp14*]) [24], for which glomerular gene expression was commonly upregulated in two models of diabetic nephropathy by microarray (ESM Table 4). Upregulation of *Tlr4* and *S100a8* gene expression in glomeruli of STZ and A-ZIP/F-1 mice was confirmed by quantitative RT-PCR (ESM Fig. 3a, b). Moreover, in STZ-HFD mice, expression of these genes was further potentiated compared with other groups such as STZ-ND and nSTZ-HFD, especially in

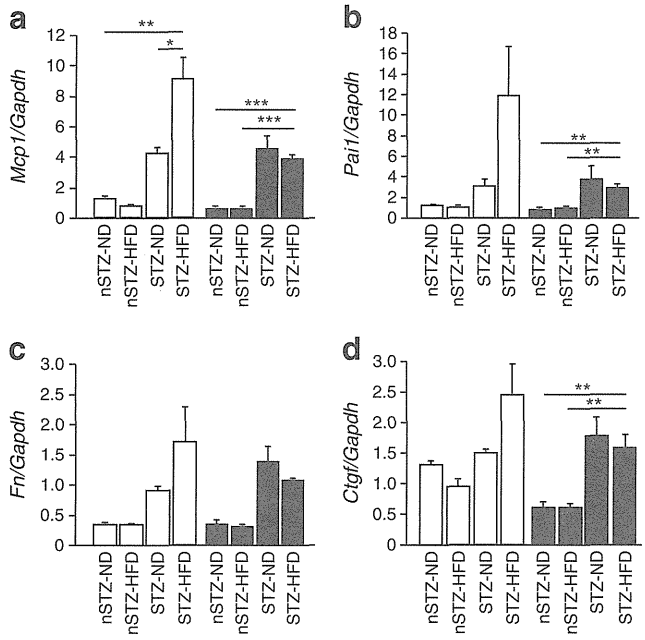

Fig. 2 Treatment with STZ and HFD synergistically upregulates inflammatory and ECM-associated gene expression in glomeruli of WT mice by real-time RT-PCR, but the effects of HFD are largely blunted in *Tlr4* KO mice: (**a**) *Mcp1*; (**b**) *Pai1*; (**c**) *Fn*; and (**d**) *Ctgf*. White bars, WT; black bars, KO. Data are means±SEM. n=4–11. *p<0.05, **p<0.01, ***p<0.001

glomeruli (Fig. 4a), but not in whole kidney (ESM Fig. 4). However, there was no significant increase in the expression of genes encoding other endogenous ligands for TLR4, such as *Hmgb1*, at the same time in both STZ and A-ZIP/F-1 mice compared with their respective controls, as assessed by microarray (ESM Table 4) or by quantitative RT-PCR (ESM Fig. 3c, d).

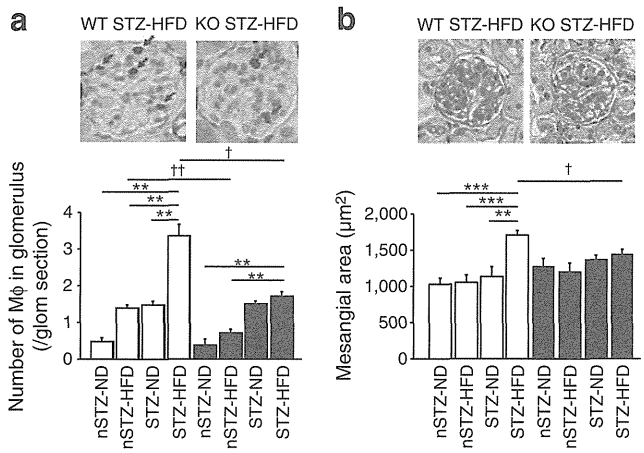

Fig. 3 Glomerular macrophage infiltration and mesangial matrix accumulation are markedly enhanced in WT mice co-treated with STZ and HFD, but not in *Tlr4* KO mice. **a** Macrophage (Mϕ) number per glomerular (glom) section determined by MAC-2 immunostaining (arrows). Magnification ×40. Data are means±SEM. n=4–5. **b** Glomerular mesangial area determined by PAS staining (purple). Magnification ×20. n=4–6. White bars, WT; black bars, KO. **p<0.01, ***p<0.001. $^{\dagger}p$<0.05, $^{\dagger\dagger}p$<0.01 for similarly treated KO vs WT

Production of S100A8 protein in diabetic kidney We performed immunohistochemical analyses of S100A8 protein in the kidneys both in STZ-HFD mice and human biopsy samples. In mice, abundance of S100A8 protein, in a punctate pattern, was observed predominantly in glomeruli of WT STZ-HFD mice, while S100A8 abundance was much lower in glomeruli of nSTZ-ND, nSTZ-HFD and STZ-ND groups (Fig. 4b, ESM Fig. 5). S100A8 protein was also detected in the interstitium of STZ-HFD mice but less abundantly than in the glomeruli. Double immunostaining revealed that 86% of S100A8 signals co-localised with macrophage marker MAC-2 in the glomeruli of STZ-HFD mice (Fig. 4c). In humans, S100A8 was abundantly detected in the glomeruli of patients with diabetic nephropathy, but not obviously in glomeruli of minor glomerular abnormality or minimal change nephrotic syndrome cases (Fig. 5).

Effects of Tlr4 defect on STZ-HFD mice and on BMDMs To elucidate a functional role played by TLR4 in the progression of diabetic nephropathy accelerated by diet-induced hyperlipidaemia, we investigated the effects of STZ and HFD in *Tlr4* KO mice. In baseline nSTZ-ND conditions, KO mice showed significantly heavier body weights compared with WT mice, paralleled by mildly elevated plasma levels of glucose, insulin, triacylglycerol and total cholesterol in KO mice (Table 1). Plasma glucose levels in KO nSTZ-HFD mice were slightly lower compared with their WT counterparts. These findings are consistent with previous observations indicating that, compared with WT mice, *Tlr4* KO mice are prone to accumulation of fat but resistant to development of insulin resistance when challenged with an HFD [25, 26]. When STZ-HFD conditions were compared between KO and WT mice, the levels of plasma glucose and total cholesterol and renal lipid deposition were similar among the genotypes, and plasma triacylglycerol levels tended to be higher in KO than WT mice (Table 1, Fig. 1b). On the other hand, exacerbation of albuminuria and suppression of glomerular podocin protein production resulting from HFD treatment in WT STZ mice were all largely blunted in KO STZ animals (Fig. 1c–f). Additionally, infiltrated macrophage counts in glomeruli and renal interstitium and mesangial expansion were remarkably smaller in KO STZ-HFD mice than in WT STZ-HFD mice (Fig. 3, ESM Fig. 2). Furthermore, upregulation of pro-inflammatory (*Mcp1* and *Pai1*), pro-fibrotic (*Fn* and *Ctgf*), *S100a8* and *S100a9* gene expression and S100A8-positive cell counts caused by HFD treatment in glomeruli of WT STZ mice were almost completely abolished in KO STZ mice (Figs 2 and 4a, b, ESM Fig. 5). These findings indicate that, despite similar degrees of metabolic abnormalities caused

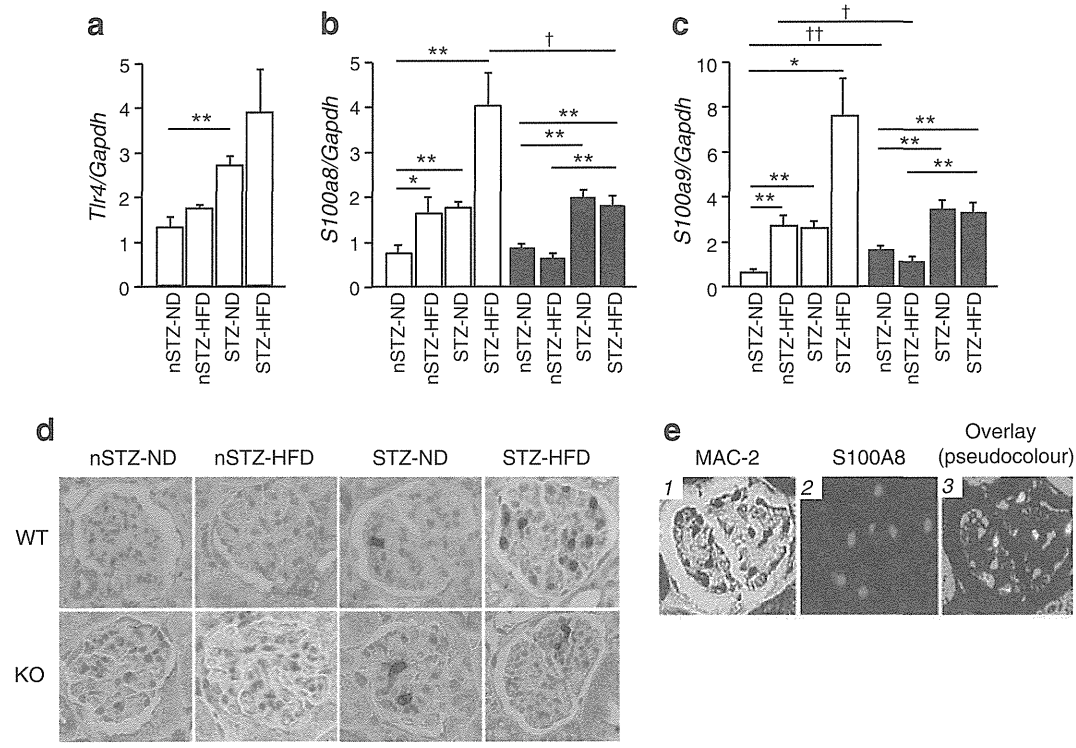

Fig. 4 Glomerular expression of *Tlr4*, *S100a8* and *S100a9* mRNA and S100A8 protein is markedly upregulated in WT STZ-HFD but not in *Tlr4* KO STZ-HFD mice, and S100A8 is predominantly produced by glomerular macrophages in WT STZ-HFD mice. **a–c** Gene expression of *Tlr4* (**a**), *S100a8* (**b**) and *S100a9* (**c**) in glomeruli, determined by real-time RT-PCR. White bars, WT; black bars, KO. Data are means± SEM. n=4–11. *p<0.05, **p<0.01. $^{\dagger}p$<0.05, $^{\dagger\dagger}p$<0.01 for similarly treated KO vs WT. **d** Glomerular S100A8 protein (brown) examined by immunohistochemistry. Magnification×40. **e** Localisation of MAC-2 (brown in panel 1, pseudocoloured with green in panel 3, by immunohistochemistry), S100A8 (red in panels 2 and 3, by immunofluorescence) and their overlaps (yellow in panel 3) in glomeruli of WT STZ-HFD mice

by diabetes and hyperlipidaemia, *Tlr4* KO mice developed much less severe renal lesions compared with WT mice.

With regard to comparison between WT and *Tlr4* KO mice treated with STZ alone (STZ-ND mice), urinary albumin excretion (Fig. 1c, d), glomerular podocin production (Fig. 1e, f), glomerular gene expression of *Mcp1*, *Pai1*, *Fn*, *Ctgf*, *S100a8*, and *S100a9* (Figs 2 and 4a), and glomerular macrophage infiltration (Fig. 3a) were all similar among two genotypes, suggesting that *Tlr4* does not strongly participate in early and mild changes of diabetic nephropathy. Concerning HFD treatment alone (nSTZ-HFD mice), there were no significant differences in urinary albumin excretion and glomerular podocin production between WT and KO mice (Fig. 1c–f), while glomerular *S100a9* gene expression (Fig. 4a) and glomerular macrophage infiltration (Fig. 3a) were significantly attenuated in KO compared with WT mice, suggesting that treatment solely with HFD significantly activated circulating macrophages in WT mice but the TLR4-mediated signal in nSTZ-HFD mice was not sufficient to cause functional changes in the glomeruli.

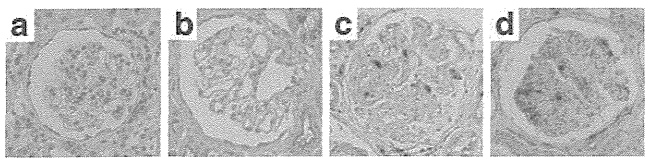

Fig. 5 S100A8 (brown) is observed in glomeruli of patients with diabetic nephropathy by immunohistochemistry: (**a**) minor glomerular abnormality; (**b**) minimal change nephrotic syndrome; and (**c**) mild and (**d**) severe cases of diabetic nephropathy

To gain insights into how the combination of diabetes and hyperlipidaemia resulted in markedly enhanced migration of macrophages into glomeruli, we examined BMDMs. We focused attention on expression of a potent TLR4 ligand, S100A8 [24]. Treatment of WT macrophages with a fatty acid, palmitate, induced *S100a8* mRNA upregulation when the cells were cultured in high-glucose conditions, but upregulation was not observed under low-glucose conditions (Fig. 6a). Furthermore, induction of *S100a8* expression by palmitate in high-glucose-treated macrophages did not occur in cells from *Tlr4* KO animals (Fig. 6b). High-glucose treatment slightly increased *Tlr4* expression in WT macrophages (Fig. 6c).

TLR4 signalling in the kidney of STZ-HFD model To examine the TLR4-downstream signalling cascade, we performed

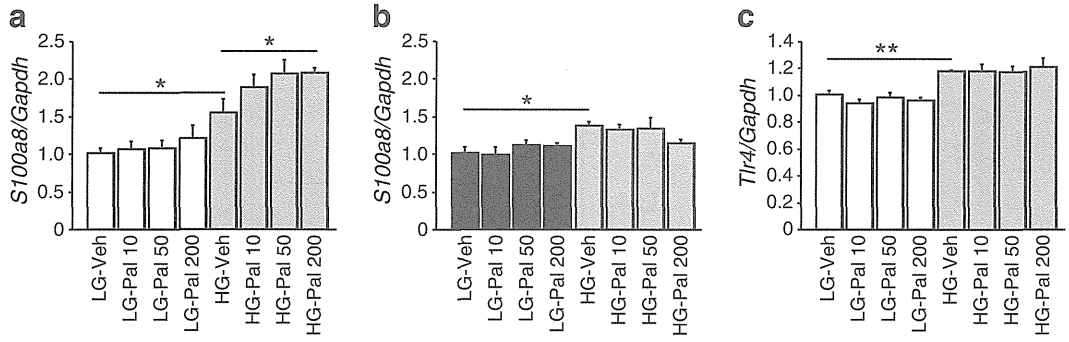

Fig. 6 *S100a8* expression in BMDMs is synergistically induced by high glucose and palmitate in a *Tlr4*-dependent manner. **a** *S100a8* mRNA expression by real-time RT-PCR in BMDMs from WT mice cultured under low-glucose (5.6 mmol/l, white bars) or high-glucose (25 mmol/l, grey bars) conditions and effects of palmitate (10–200 μmol/l). Data are means±SEM. $n=6$. **b** *S100a8* mRNA expression in BMDMs from *Tlr4* KO mice cultured under low-glucose (black bars) or high-glucose (grey bars) conditions and the effects of palmitate. $n=6$. **c** *Tlr4* mRNA expression in WT BMDMs. $n=6$. $^{*}p<0.05$, $^{**}p<0.01$. LG, low glucose; HG, high glucose; pal, palmitate; Veh, vehicle

western blot analyses of key adaptor proteins and transcription factors which have been reportedly classified into myeloid differentiation primary response gene (88) (MYD88)-dependent, TIR-domain-containing adapter-inducing interferon-β (TRIF)-dependent or common pathways (Fig. 7a) [7], using whole kidney lysate. Treatment of WT STZ mice with HFD was associated with increased phosphorylation of inhibitor of κB (IKB) and c-Jun N-terminal kinase (JNK) in a common pathway, and with increased phosphorylation of interferon regulatory factor 3 (IRF3) in a TRIF-dependent pathway, but not with increased protein production of TNF receptor-associated factor 6 (TRAF6) nor increased phosphorylation of interleukin-1-receptor-associated kinase (IRAK) in the MYD88-dependent pathway (Fig. 7b–e). PCR array analysis, which allows simultaneous evaluation of relevant genes involved in the signalling cascades of TLR1–TLR9, confirmed that in WT STZ-HFD kidneys, TRIF-dependent pathway-inducible genes (*Cxcl10*, *Ifnb1* [encoding interferon β1] and *Cd80*) and common pathway-inducible genes (*Mcp1*) were highly upregulated, but genes involved in the MYD88-dependent pathway (*Cd14*, *Ly96* [encoding myeloid differentiation protein-2 {MD-2}], and *Traf6*) were not changed compared with WT STZ-ND kidneys (ESM Table 5). Furthermore, disruption of the *Tlr4* gene markedly blocked the activation of the putative TLR4 downstream signalling cascade in STZ-HFD mice (Fig. 7b–e, ESM Table 5).

Discussion

In the present study, we have revealed that treatment of WT mice with STZ combined with HFD synergistically aggravated renal lesions, indicated by enhancement of albuminuria, macrophage infiltration, mesangial expansion and pro-inflammatory/ECM-associated gene induction in glomeruli. These changes were accompanied with upregulation of a TLR4 ligand, S100A8, and activation of putative TRIF-dependent pathway downstream of TLR4. In *Tlr4* KO mice, the addition of HFD to STZ had almost no effect on kidney damage, suggesting that TLR4 plays an important role in the exacerbation of diabetic nephropathy by hyperlipidaemia.

Of note, treatment with STZ alone caused similar and mild renal changes in WT and KO mice, suggesting that the TLR4 signal may not significantly participate in the onset of diabetic nephropathy at 8 weeks after STZ injection [13]. However, WT mice fed with HFD (nSTZ-HFD) exhibited significantly higher levels of *S100a9* gene expression and more macrophage infiltration in glomeruli compared with KO mice, but these effects were not reflected in differences in other renal lesion variables, suggesting that macrophage activation in nSTZ-HFD mice may require longer observation periods than were used in this study in order to be functionally relevant.

Here, to study the effects of an HFD on diabetes, we used a lean model of type 1 diabetes to avoid introducing complexity through alterations in insulin resistance and fat accumulation with the HFD or by *Tlr4* gene disruption in the type 2 diabetes model [19, 20]. The HFD-induced and hypertriacylglycerolaemia-associated renal injury observed in this study may have been caused through activation of TLR4 by NEFA [25, 26], oxidised LDL [27], or triacylglycerol-rich lipoproteins [6]. Previous studies have proposed that, by direct lipotoxicity on tubular epithelial cells, diet-induced obesity alone is sufficient to cause inflammatory and fibrotic changes in the whole kidney preparations through gene expression of *Cd36* or *sterol regulatory element-binding protein-1c* (*Srebp1c*) [28–30]. In the present study, however, treatment of WT mice solely with HFD resulted in very mild renal lesions, probably because we used a diet with a lower fat content and studied the mice for a shorter period of time compared with earlier reports [28–30]. Furthermore, HFD increased glomerular *Cd36* mRNA expression but STZ-induced

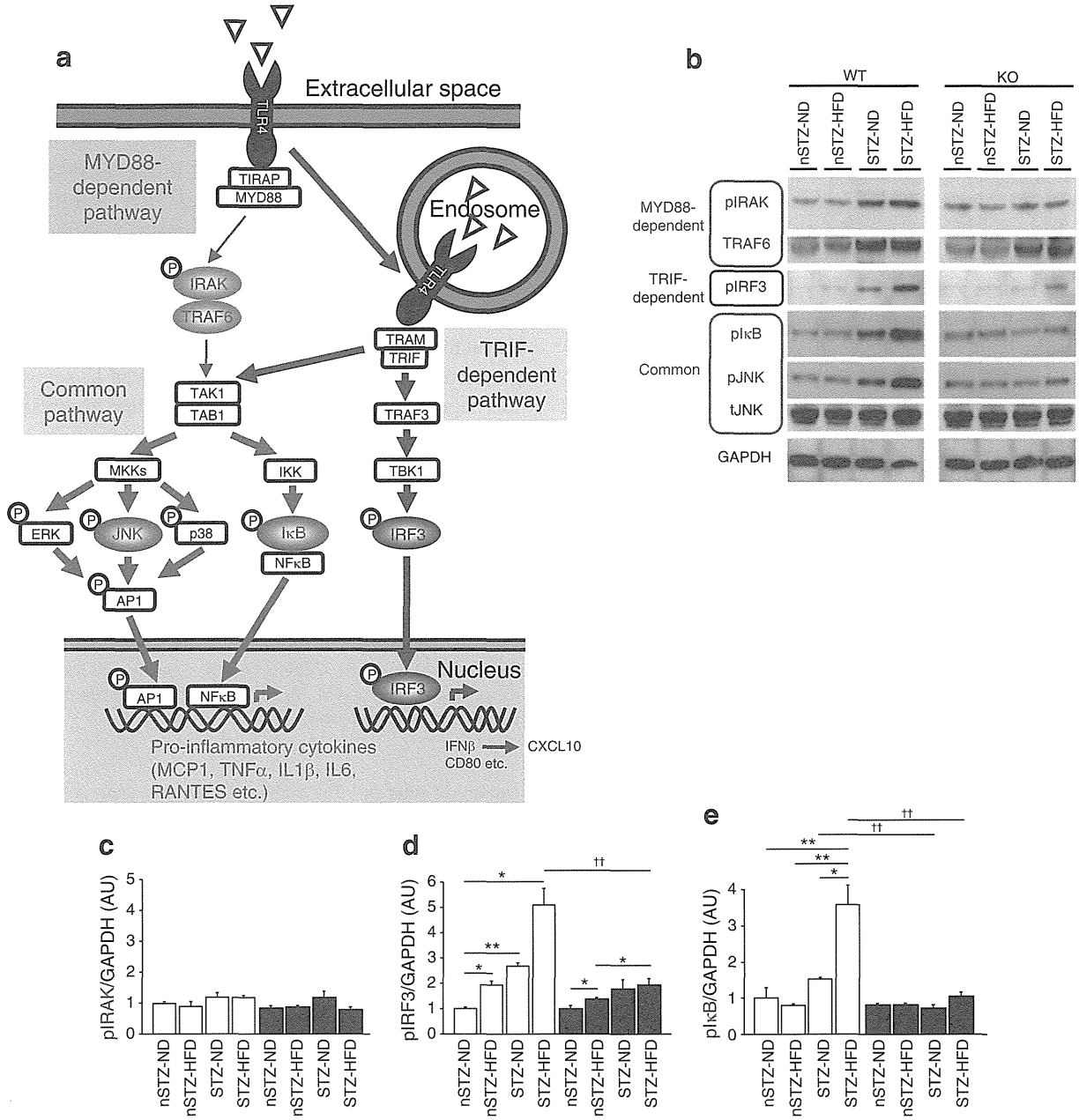

Fig. 7 Exacerbation of STZ-induced diabetic nephropathy by HFD is associated with increased phosphorylation of proteins involved in TRIF-dependent and common pathways of the TLR4 signalling cascade in WT kidney but not in *Tlr4* KO kidney. **a** Schema describing the known TLR4 signalling cascade. The common pathway can be activated both through MYD88-dependent and TRIF-dependent pathways. Key molecules analysed in (b) are highlighted as elliptical objects. **b-e** Western blot analyses of TLR4 signalling and quantitative evaluation. White bars, WT; black bars, KO. Data are means±SEM. $n=4$. $^{*}p<0.05$, $^{**}p<0.01$. $^{\dagger\dagger}p<0.01$ for similarly treated KO vs WT. AP1, jun proto-oncogene; AU, arbitrary units; CXCL10, chemokine (C-X-C motif) ligand 10; ERK, mitogen-activated protein kinase 1; (p)IKB, (phosphorylated) inhibitor of κB ; IKK, inhibitor of kappa light polypeptide gene enhancer in B cells, kinase; (p)IRAK, (phosphorylated) interleukin-1 receptor-associated kinase 1; pIRF3, phosphorylated IRF3; (p)/(t)JNK, (phosphorylated)/(total) JNK; MKKs, mitogen-activated protein kinase kinases; p38, mitogen-activated protein kinase 14; RANTES, chemokine (C-C motif) ligand 5; TAB1, TGFβ-activated kinase 1/MAP3K7 binding protein 1; TAK1, nuclear receptor subfamily 2, group C, member 2; TBK1, TANK-binding kinase 1; TIRAP, Toll-interleukin 1 receptor domain containing adaptor protein; TRAF3, TNF receptor-associated factor 3; TRAM, translocation associated membrane protein 1

diabetes reduced it, and glomerular *Srebp1c* expression was decreased both by HFD and STZ (ESM Fig. 6), indicating that HFD-induced exacerbation of diabetic nephropathy cannot be explained by upregulation of CD36 or SREBP1C.

S100A8 forms a heterodimer with S100A9, and the complex is one of the most powerful endogenous ligands for TLR4, which is essential for full activation of macrophages and other leucocytes, by a positive feedback loop, during

endotoxin-induced shock and vascular and autoimmune disorders [24, 31, 32]. TLR4 signalling also plays an important role in the development of various kidney diseases, yet the role of TLR4 in diabetic glomerulopathy or hyperlipidaemia-induced kidney damage remains to be elucidated [8–13]. Recently, Burkhardt et al and Bouma et al reported that serum S100A8/A9 complex concentrations were elevated in patients with diabetes [33, 34]. In our study, S100A8 protein was abundant in the glomeruli of mice given STZ and HFD and also in glomeruli of patients with diabetic nephropathy, and was mainly produced by macrophages. Furthermore, we found that high glucose and NEFA treatments, when combined, markedly upregulated *S100a8* expression in WT macrophages, but not in *Tlr4* KO macrophages. These findings suggest that production of S100A8 is not just an indicator of systemic inflammation but may play a pathogenic role in the deterioration of diabetic nephropathy. Functional analysis of S100A8 protein production in diabetic mice is currently under way in our laboratory. Candidate *Tlr4*-expressing cells in the diabetic kidney include macrophages, podocytes and mesangial and tubular epithelial cells [8, 9]. So far, we have been unable to obtain reliable findings by immunohistochemistry using commercially available antibodies for TLR4, and we are now trying other methods. Of note, upregulation of *S100a8* gene expression by HFD in STZ mice was also observed in the liver and aorta, suggesting that the effects of these treatments are not specifically targeted to the kidney but are systemic (ESM Fig. 6). HMGB1 is one of endogenous ligands of TLR4 [9], and AGE-specific receptor (AGER or RAGE) is one of the S100A8 receptors so far identified [35]. Although mRNA expression of these molecules in glomeruli was not upregulated in diabetic mice in this study (ESM Fig. 3, ESM Table 4), we cannot exclude the possibility that they are involved in hyperlipidaemia-induced renal injury.

The macrophage has been presumed to be a critical mediator of diabetic nephropathy [36–38], and blockade of the MCP-1/CC chemokine receptor 2 system in diabetic mice leads to reduced albuminuria, mesangial expansion and macrophage infiltration [39–42]. Secretory factors from macrophages may cause histological and functional changes in glomeruli. For example, TGF β1 (TGFB1) and MCP1, induced in surrounding cells by or secreted directly from activated macrophages, have been shown to upregulate CTGF production [43] and increase albumin permeability in cultured podocytes [44–46]; we have recently reported that overproduction of CTGF specifically in podocytes is sufficient to worsen diabetic nephropathy [19].

Downstream signalling of TLR4 has been divided into MYD88-dependent and TRIF-dependent pathways, leading to early- and late-phase nuclear factor of κ light polypeptide gene enhancer in B cells 1 (NFκB) activation, respectively [7]. In addition, endocytosed TLR4 activates the TRIF-dependent pathway [47]. It is interesting to determine whether pathologically accumulated lipids in endosomes of macrophages can cause chronic inflammation via the TRIF-dependent pathway in the kidneys of STZ-HFD mice. Here, in STZ-HFD kidneys, we observed an increase in IRF3 protein phosphorylation and *Cxcl10*, *Ifnb1* and *Cd80* mRNA expression, reported to be in the TRIF-dependent pathway, but experiments blocking TRIF activity are required to demonstrate the TRIF dependency of the process.

In conclusion, we have elucidated a novel mechanism of hyperlipidaemia-induced renal damage in diabetic conditions in a TLR4-dependent manner that appears to involve the activation of a S100A8/TLR4 signalling pathway in glomeruli. Further investigation is required to see whether this signalling cascade is relevant in the progression of nephropathy in diabetic patients.

Acknowledgements We acknowledge S. Akira (WPI Immunology Frontier Research Center, Osaka University, Suita, Japan) for kindly providing us with *Tlr4* KO mice. We gratefully acknowledge Y. Ogawa and A. Yamamoto and other laboratory members for their assistance.

Funding This work was supported in part by Grant-in-Aid for Diabetic Nephropathy Research (K. Mori), research grants from the Japanese Ministry of Education, Culture, Sports, Science and Technology (T. Kuwabara, K. Mori and M. Mukoyama) and from the Smoking Research Foundation (M. Mukoyama).

Duality of interest The authors declare that there is no duality of interest associated with this manuscript.

Contribution statement All authors contributed to the conception and design, or analysis and interpretation of data, and drafting the article or revising it critically for important intellectual content, and have given final approval of the version to be published.

References

1. Maisonneuve P, Agodoa L, Gellert R et al (2000) Distribution of primary renal diseases leading to end-stage renal failure in the United States, Europe, and Australia/New Zealand: results from an international comparative study. Am J Kidney Dis 35:157–165
2. Decleves AE, Sharma K (2010) New pharmacological treatments for improving renal outcomes in diabetes. Nat Rev Nephrol 6:371–380
3. El-Atat FA, Stas SN, McFarlane SI, Sowers JR (2004) The relationship between hyperinsulinemia, hypertension and progressive renal disease. J Am Soc Nephrol 15:2816–2827
4. Perkins BA, Ficociello LH, Silva KH, Finkelstein DM, Warram JH, Krolewski AS (2003) Regression of microalbuminuria in type 1 diabetes. N Engl J Med 348:2285–2293
5. Ravid M, Brosh D, Ravid-Safran D, Levy Z, Rachmani R (1998) Main risk factors for nephropathy in type 2 diabetes mellitus are plasma cholesterol levels, mean blood pressure, and hyperglycemia. Arch Intern Med 158:998–1004
6. Rutledge JC, Ng KF, Aung HH, Wilson DW (2010) Role of triglyceride-rich lipoproteins in diabetic nephropathy. Nat Rev Nephrol 6:361–370